$Y = Y_C + P \times$

MARINE PHYSICAL LABORATORY, 0701
of the Scripps Institution of Oceanography
San Diego, California 92152-6400

Technical Memorandum **AV11-018t**
To: Atmospheric Optics Group 23 August 2011
From: M. E. Karr and J. E. Shields
Subject: Transmittance Results from Slant Path Transmittance Algorithm Version 1

In Memo AV11-016t "Logic for Slant Path Transmittance Algorithm Version 1", we documented the logic for the first version of the new Slant Path Transmittance algorithm, which we are calling TrAlg. Memo AV11-017t "Program TrAlg Version 1, Slant Path Transmission Algorithm" documents the software. In this memo, we document sample transmittance results. These tests serve both to verify that the algorithm is reasonable, and also to show under what conditions the slant path transmittance should be acceptable for obtaining a propagation of better than 50%. In all cases, I have tried to run the tests with reasonable inputs, i.e. inputs ranging over the range of expected conditions.

1. Input Values

Fig. 1 shows a typical vertical profile of total volume extinction or scattering coefficient. (Since these studies are done in visible wavelengths with insignificant absorption, we have used either term interchangeably.)

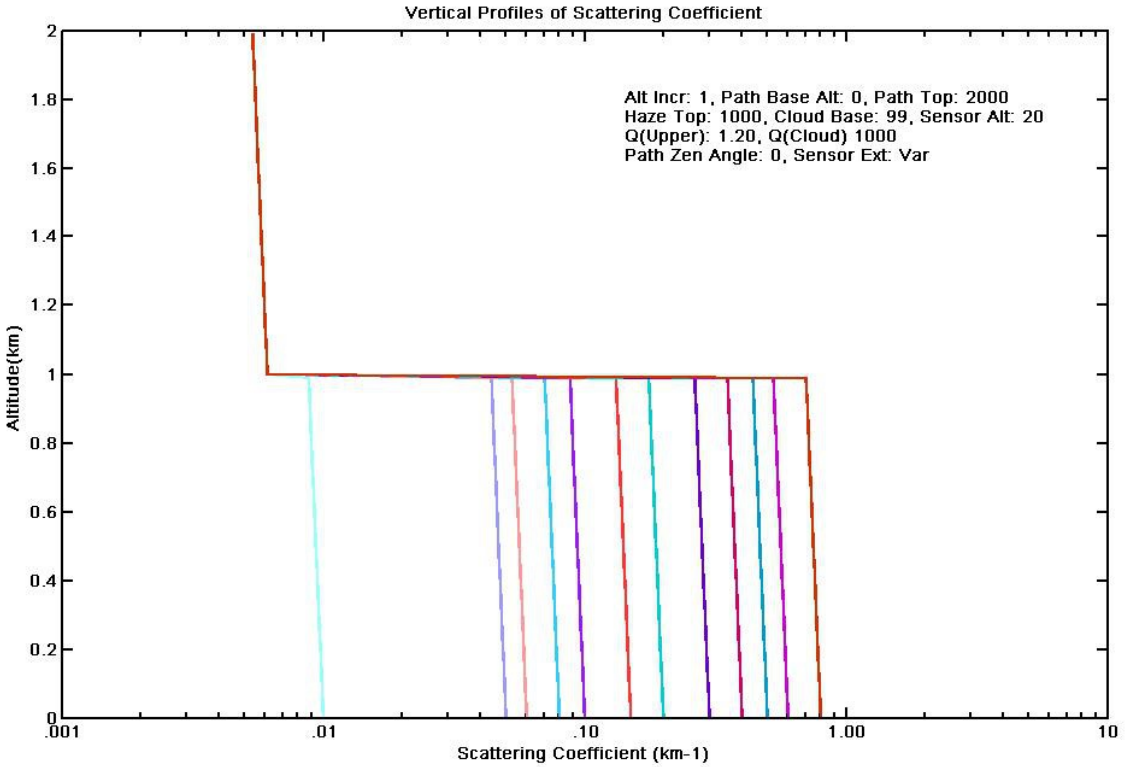

Fig. 1. Vertical Profile for Total Volume Extinction or Scattering Coefficient for a range of input extinction coefficients at 20 m sensor altitude, and a fixed haze top, with no clouds

In this figure, we have indicated the significant algorithm inputs in the header. The base altitude is 0 m, the path top is 2000 m, the haze top is 1000 m, the cloud base is 99 (meaning no clouds), the sensor altitude is 20 m, the mixing ratio Q for the upper layer above the haze is 1.2, the mixing ratio Q for the clouds is set at 1000 (but not used, since the cloud base is 99), the path zenith angle is 0, and the sensor extinction at 20 m is variable, but given in the x axis.

I will put the plots of results for all of the case studies at the end of the memo, and discuss all the results here. For each variable that was evaluated, I will show both a log and a linear plot of transmittance, as I feel they complement each other in giving the analyst a feel for the results. All calculations were made for a red filter, and the haze layer extinction is normalized with respect to the red extinction.

2. Results without Clouds

Figs. 2 and 3 show the resulting transmittance for the zenith angles 0 (overhead), 60, and 85 (near the horizon). Visibility is given by 3/s, where s is the photopic scattering coefficient. Typically the red scattering or extinction coefficient is slightly less than the photopic scattering or extinction coefficient. We have shown red extinction ranging from .01 km^{-1} to 1 km^{-1}, so this corresponds to visibilities a bit less than 300 km to 3 km. The lower value is the round number closest to the Rayleigh limit. Most realistic situations will lie between extinctions of about .05 km^{-1} to 1 km^{-1}, or 60 km to 3 km. Under these conditions, we see in Figs. 2 and 3 that the vertical beam transmittance between 0 and 2 km altitude remains above 50% under all but the highest extinctions. However the transmittance decreases, as expected, as the path of sight drops to lower angles. At 85°, the beam transmittance drops below 50% at a sensor extinction of about .06 km^{-1} (visibility about 50 km), and below 10% at a sensor extinction of about .25 km^{-1} (visibility about 12 km).

Figs. 4 and 5 show similar results, although in this case the results are plotted as a function of zenith angle, for extinctions of .08, .3, and .6 km^{-1}. These imply visibilities slightly less than 37.5, 10, and 5 km. As anticipated, the transmittances drop quickly near the horizon.

However, these paths near the horizon may not be realistic for the scenarios of interest to the Navy. In particular, a path of sight with a top at 2000 m and an angle of 85° is quite long. At 0° zenith angle the path length is 2000 m; at 60° it increases to 4000 m, and at 85°, it increases to 23,000 m. So perhaps a more relevant question for angles near the horizon is what the impact of increasing path length is.

Figs. 6 and 7 show what happens as the path length increases from 500 m to 5000 m, for paths near the horizon at 70°, 80°, 85°, and 88°. These plots all hold the extinction at .3 km^{-1} for a visibility of about 10 km. In all cases the transmittance drops below 50% by the time the path length is 5000 m. However, for these reasonably clear conditions, none of the angles results in a transmittance less than 10%. In the case of the 70° path, there is an abrupt change in the rate of decrease, because this path pops out above the top of the haze, and after

that there is little change. The paths at 80° and below continue to have decreasing transmittance with increasing path length, because they remain within the haze layer.

In most of the test calculations, I let the haze top vary between 0 and 3 km. Our group measured scattering coefficient profiles on over 200 flights in the continental US, Europe, and Asia. A quick look through several of the reports on these data showed that most of the time the haze top fell within these ranges. As Figs. 8 and 9 show, the impact of the height of the haze top can be fairly significant. These calculations were for a path top of 3 km. Figs. 10 and 11 show the impact for a longer path, with a path top of 10 km. It is the left side of this plot that is most relevant, because the right side shows haze tops ranging up to 10 km, which is not apt to happen.

In the absence of clouds, these are the primary variables for our study. Allowing the Q to vary for the upper clear layer has almost no impact, as the upper layer contributes such a small amount to the total. As an example, consider the case of the haze top at 1000 m, the path top at 3000 m, the extinction at .3 km^{-1}, and the zenith angle of 60°, which is one of the cases shown in Fig. 8. In this example, the haze layer vertical transmittance is .754; the upper layer vertical transmittance is .989; the net vertical transmittance is .746; and the slant path transmittance is .557. That is, the haze contributes nearly all the losses even though it occupies only a third of the path. Changing the Q value for the upper level would only change the .989 value a small amount, and this would have little impact on the path transmittance.

3. Results with Clouds

Clouds naturally have a very significant impact on the transmittance. In Figs. 12 through 15, we show the results for several cloud types. To generate these data, we selected data from the Appendix of Memo AV11-016t, choosing the average Q value and cloud base that are typical of five cloud types. These cloud types are thin cirrus, thick cirrus, alto-stratus, cumulus, and nimbo-stratus. The cloud characteristics are shown in Table 1. The results are shown for a vertical path in Figs. 12 and 13, and for a path at 60° zenith angle in Figs. 14 and 15. In each case we have used a haze top of 1000 m, and a sensor extinction of .3 km^{-1}.

Table 1
Input Values for Cloud Layers

Cloud Type	Cloud Base	Mixing Ratio Q
Thin Cirrus	6000 m	250
Thick Cirrus	6000 m	440
Alto Stratus	3000 m	1950
Cumulus	1000 m	1500
Nimbo Stratus	1000 m	4300

The program does not currently include the ability to input a cloud top. In order to handle this, I changed the path top. In the case of the cirrus clouds, I set the cloud base to 6000 m, and then set the path top to values of 6000 m, 6100 m, 6200 m, … to 7000 m. Similarly, for

alto-stratus, with a base of 3000 m, the path top varied from 3000 to 4000 m, and with both cumulus and nimbo-stratus, with a base of 1000 m, the path top varied from 1000 to 2000 m. Thus in all cases we kept the haze and upper clear layers fixed for each cloud type, and added a cloud layer varying from 0 to 1000 m in thickness.

I should also note, before we compare the results for different clouds, that because the cloud bases vary, the upper clear layer ranges from a thickness of 0 to 5000 m. This has a very small impact however. The transmittance of the upper clear layer is 1.00 when the thickness is 0, and when the thickness is 5000 m, the transmittance of the upper clear layer is .98 at 0°, and .96 at 60°. Thus we can proceed with an evaluation of the impact of the clouds.

In Figs. 12 through 15, we note that the curves for the alto-stratus and the cumulus nearly overlay each other. The Alto-stratus has a slightly higher Q value (which did surprise me), but it is offset by the lower Rayleigh scattering at the higher altitude, yielding nearly the same results as the cumulus. If we use a higher Q value for the cumulus, it will decrease the transmittance.

Evaluating Figs. 12 and 13, which is the case for the vertical path of sight, we see that there are cirrus cases with thin cloud layers that result in transmittances less than 50%. This means that we will definitely need to add the ability to input cloud top to the algorithm, as some of these cases may be of interest. The blooming may prevent such a path of sight from being useful for a laser weapon, but it may not prevent such a path of sight from being useful for detection. In general however, the transmittance through the clouds drops quite low. Even for the thin cirrus, it is below 50% for layers thicker than about 600 m. For the low and mid-altitude cloud types, the vertical transmittance drops below 10% at layer thicknesses of 300 m or less.

In Figs. 14 and 15, which show the same cases for a path of sight at 60° zenith angle, we see that even at this moderate angle, the path transmittance is quite low. For thin cirrus, the transmittance drops below 50% before a thickness of 100 m is reached. For the lower and mid-altitude cloud types, the transmittance drops to 10% near a thickness of 100 m.

4. General Comments

The fact that the upper clear layer has very little effect, because the transmittance in this layer is so high, means that uncertainties in the Q value do not have a large impact. We also find that the uncertainties in the Q values within the clouds will not have a large impact, except for thin layers of thin cirrus, because these paths are pretty much unusable. However, the presence or absence of clouds is a very strong driver, so for this scheme to work, we need to know whether clouds are present, either from visual observation or a ceilometer.

For a given path geometry in the absence of clouds, the magnitude of the sensor extinction is the strongest driver. This is the reason that I feel it's reasonable to provide estimates of slant path transmittance given a measured sensor extinction. They will not be exact, but they should be reasonable estimates under most conditions. The height of the haze transition and

the presence is the next most important driver, and we hope this can be obtained from weather reports or the ceilometer data.

Obviously look angle and path length are strong drivers, but these should be known in a given scenario.

These results should be reasonably valid for the short wave IR (SWIR) as well as the visible wavelengths, in the regions such as 1.064 that have minimal absorption. Fig. 16 shows the modeled relationship between the SWIR and various visible wavelengths, from Memo AV09-038t "SWIR Extinctions, Modeling and First Images". One way that this discussion changes is that we need to use the term "extinction" exclusively when we are discussing the SWIR. And when we say that the visibility would be "about 10 km", for example, it would be a bit lower than that. This is because the SWIR extinctions tend to be a bit lower than photopic or red, and thus the 3/s or 3/α estimate for visibility from the SWIR is too high. However, the relationships shown in these examples between transmittance and extinction should be independent of the wavelength.

Although this study shows the impact of trends, this is not our only goal. We want to determine the transmittance at a given point in time in a given direction. For this, we plan to enhance the current algorithm with ceilometer data to provide a better estimate of clouds and heavy haze. This will follow in another generation of the algorithm.

In summary, we feel that this algorithm provides reasonable results for the slant path transmittance as a function of the sensor extinction and other parameters such as the height of the haze layer. As a stand-alone program, it's not terribly useful except for case studies such as we have shown. However, if this code were integrated into software that includes real-time knowledge of the path to a moving target, we feel that this could be a vital part of a decision aid. It could be used in testing, to interpret the observability of a target and the anticipated influence of extinction on the flux on the target. And in operational use it could be used in a tactical decision aid to support decisions regarding weapon dwell time on target.

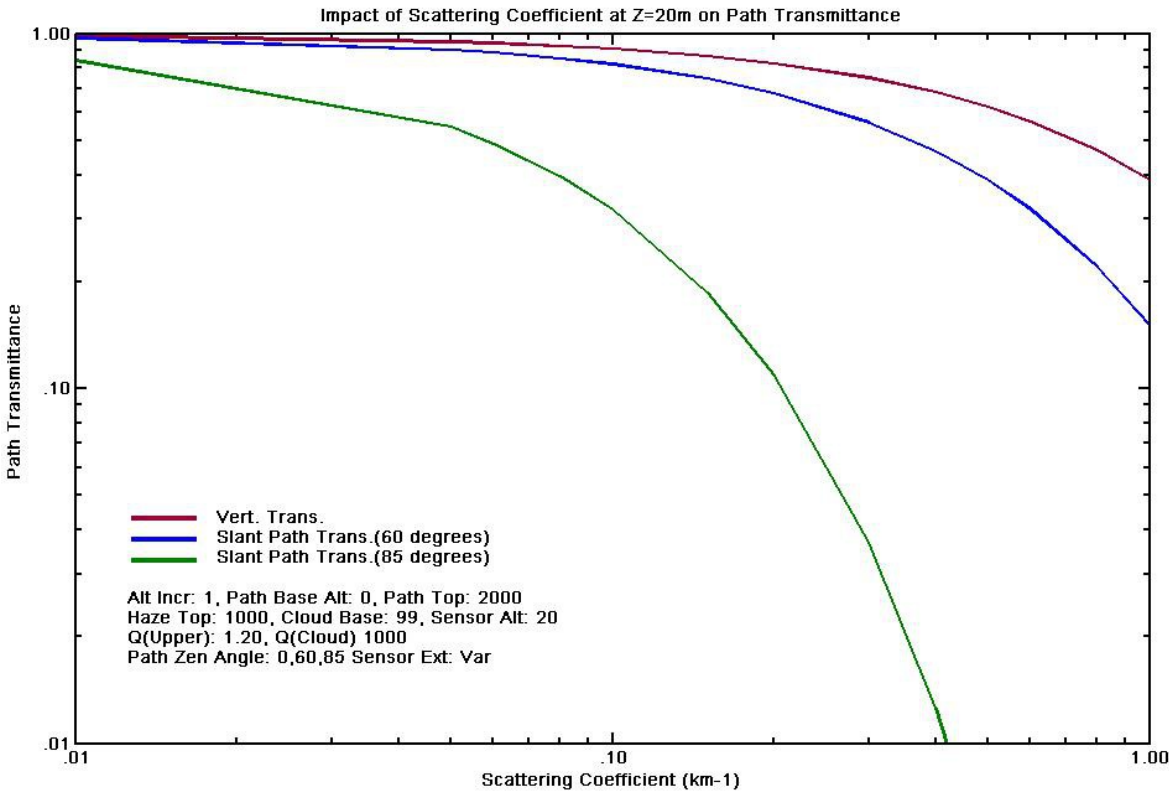

Fig. 2. Log plot showing impact of varying Sensor Extinction for look angles 0°, 60°, and 85°

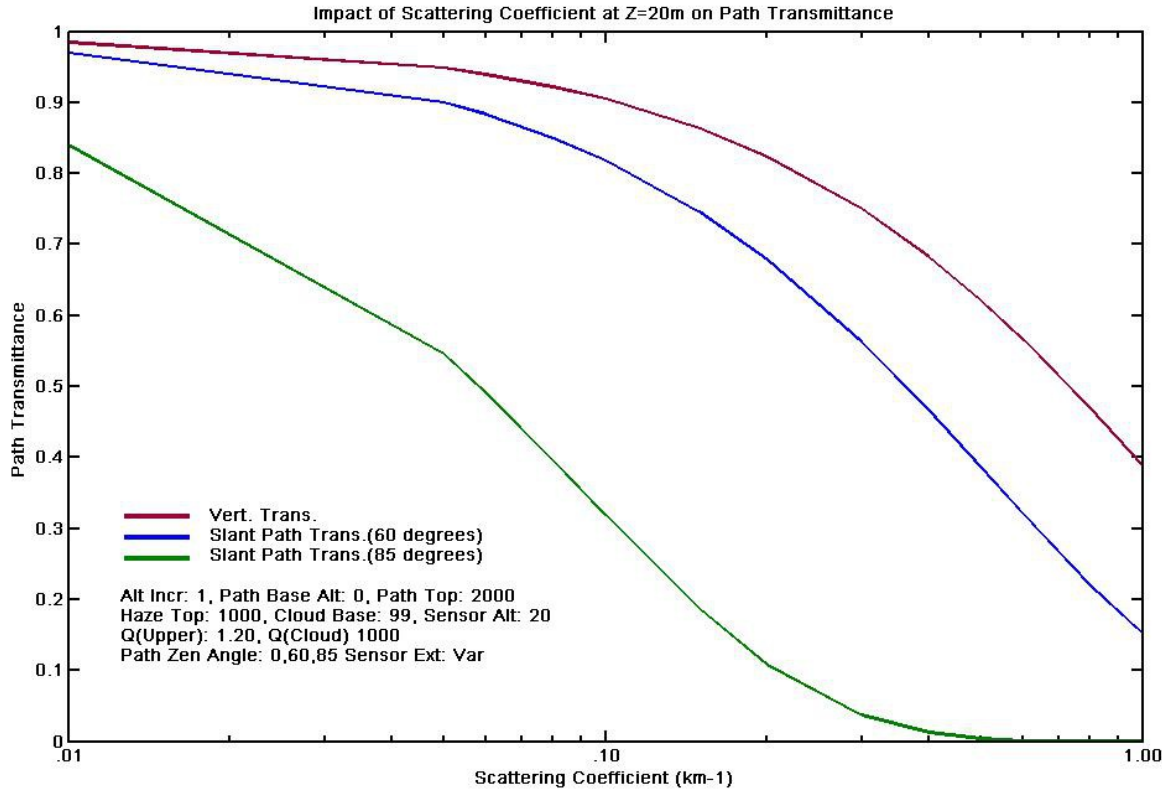

Fig. 3. Linear plot showing impact of varying Sensor Extinction for look angles 0°, 60°, and 85°

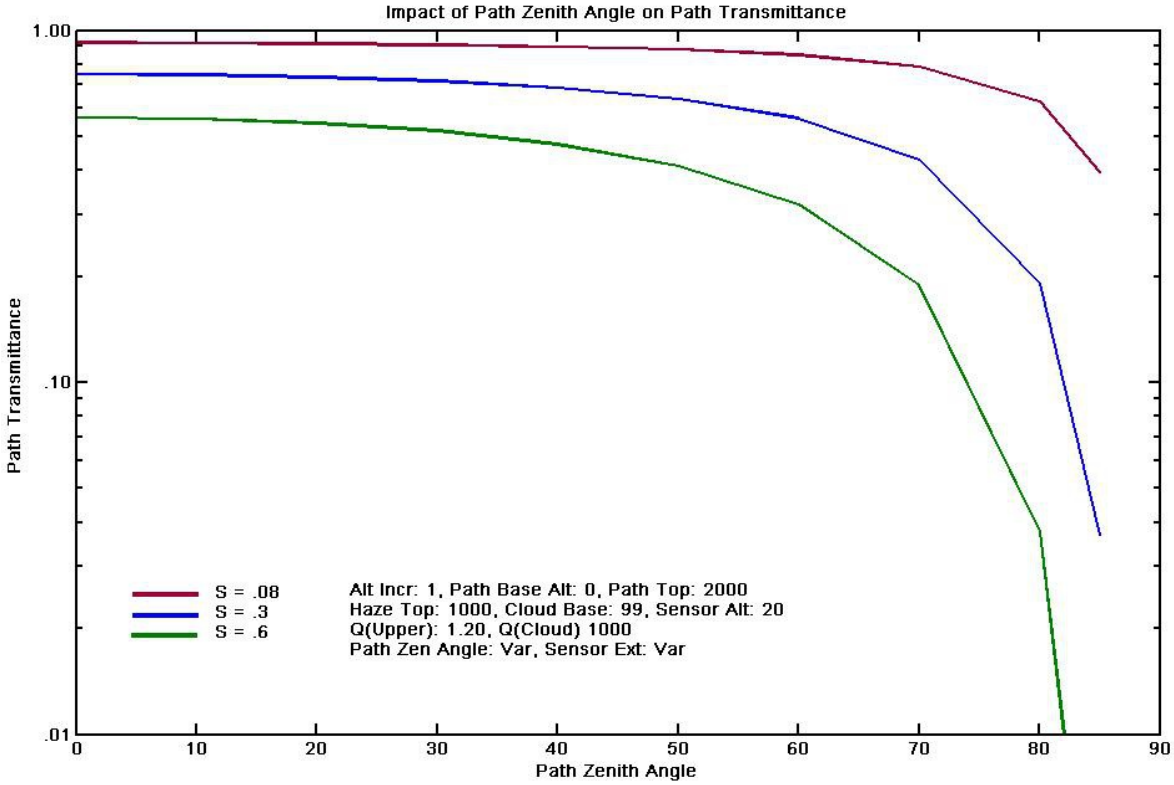

Fig. 4. Log plot showing impact of varying Zenith Angle for Extinctions .08, .3, and .6 km^{-1}

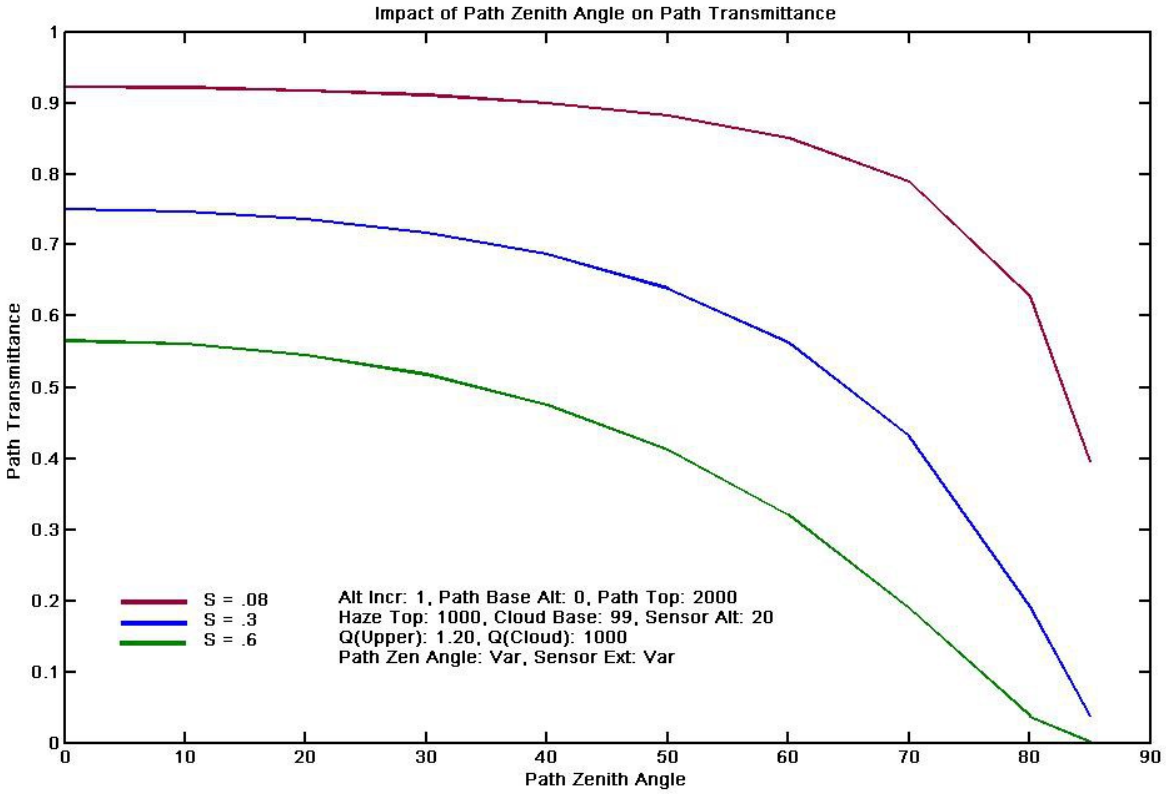

Fig. 5. Linear plot showing impact of varying Zenith Angle for Extinctions .08, .3, and .6 km^{-1}

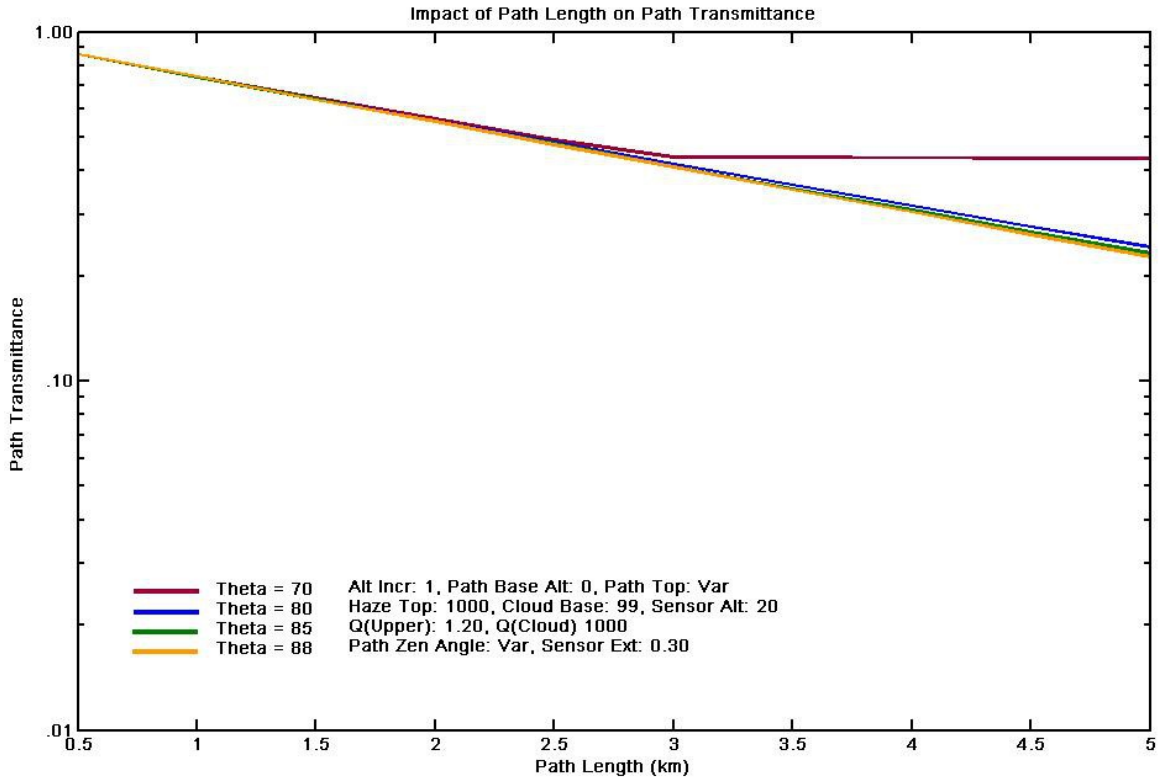

Fig. 6. Log plot showing impact of varying Path Length for Zenith Angles 0°, 60°, and 85°

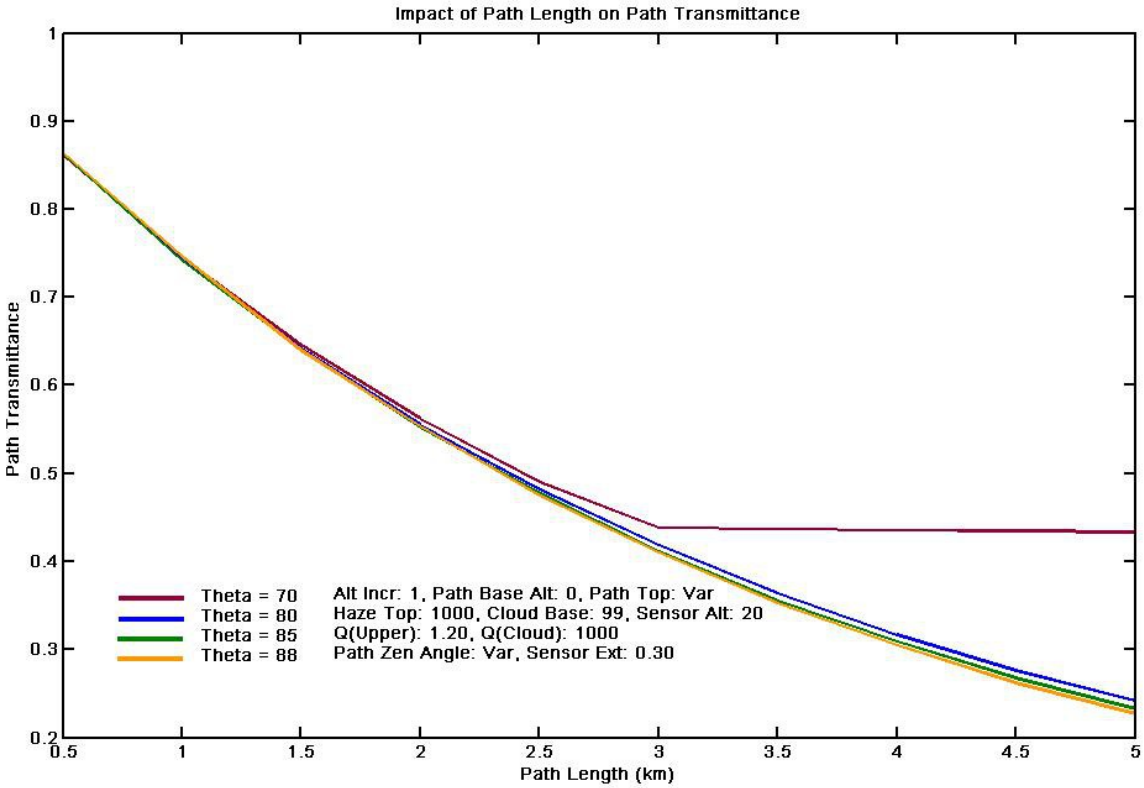

Fig. 7. Linear plot showing impact of varying Path Length for Zenith Angles 0°, 60°, and 85°

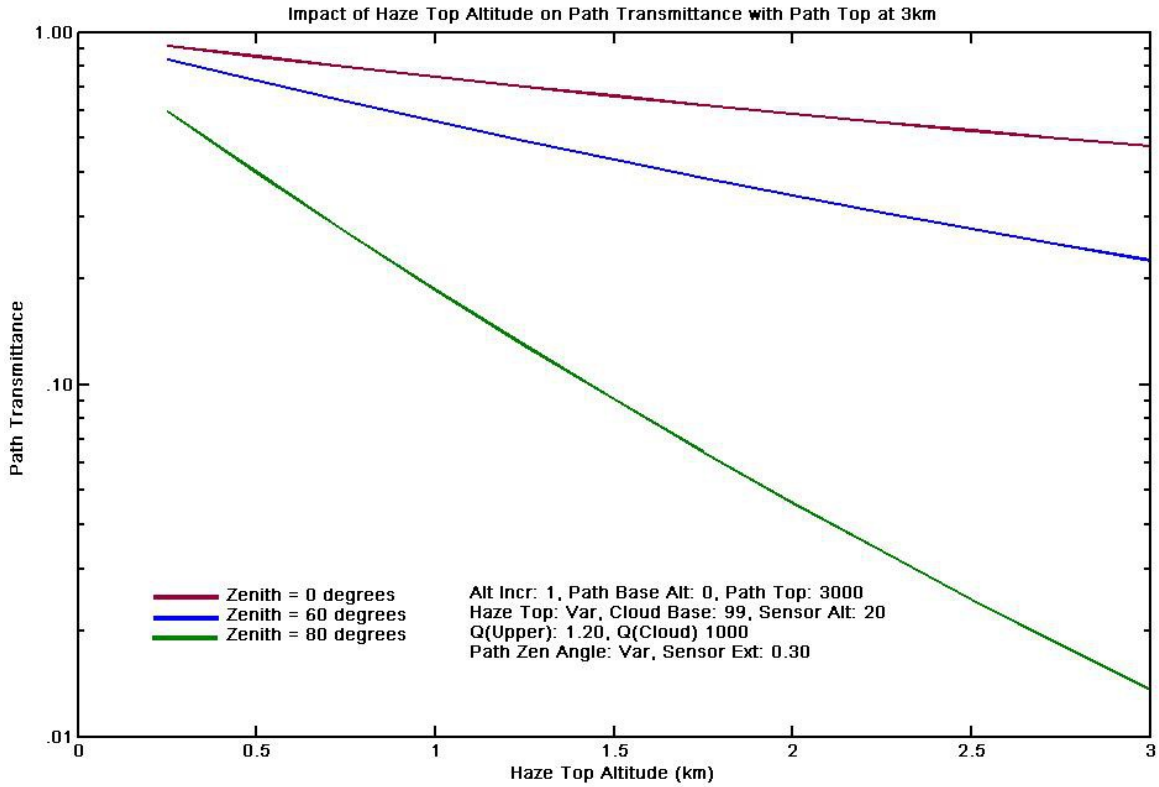

Fig. 8. Log plot showing impact of varying Haze Top for a Path Top of 3 km and for Zenith Angles 0°, 60°, and 85°

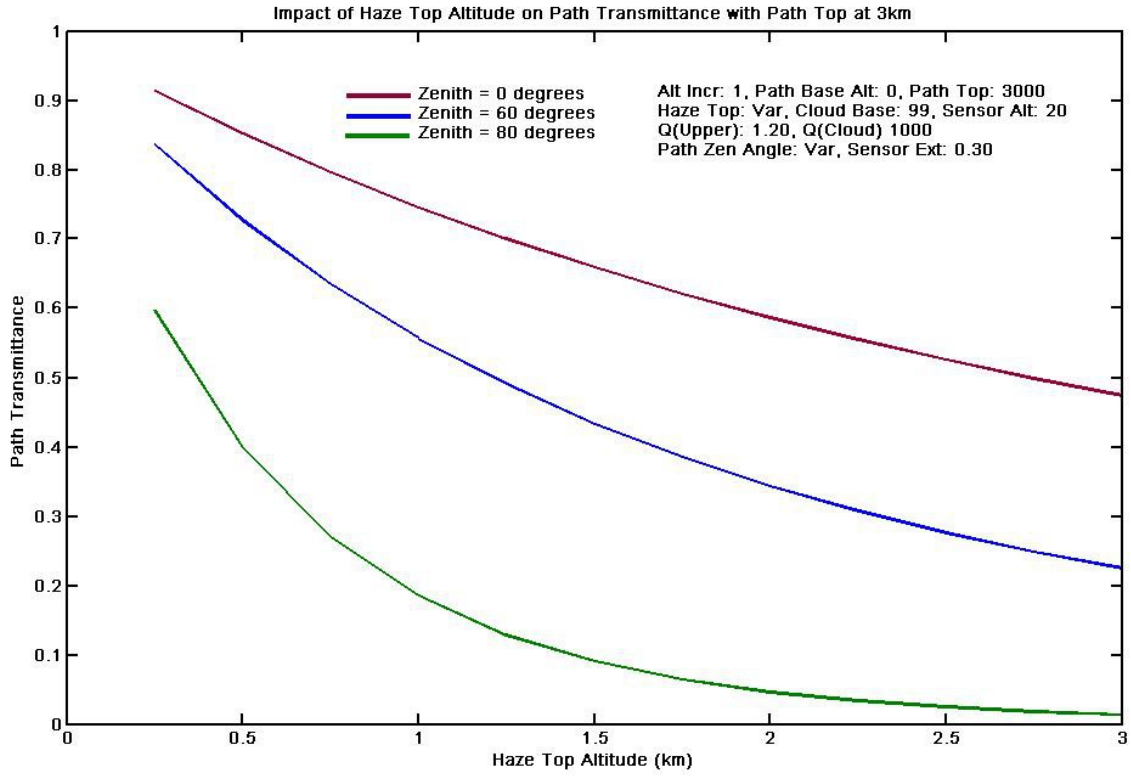

Fig. 9. Linear plot showing impact of varying Haze Top for a Path Top of 3 km and for Zenith Angles 0°, 60°, and 85°

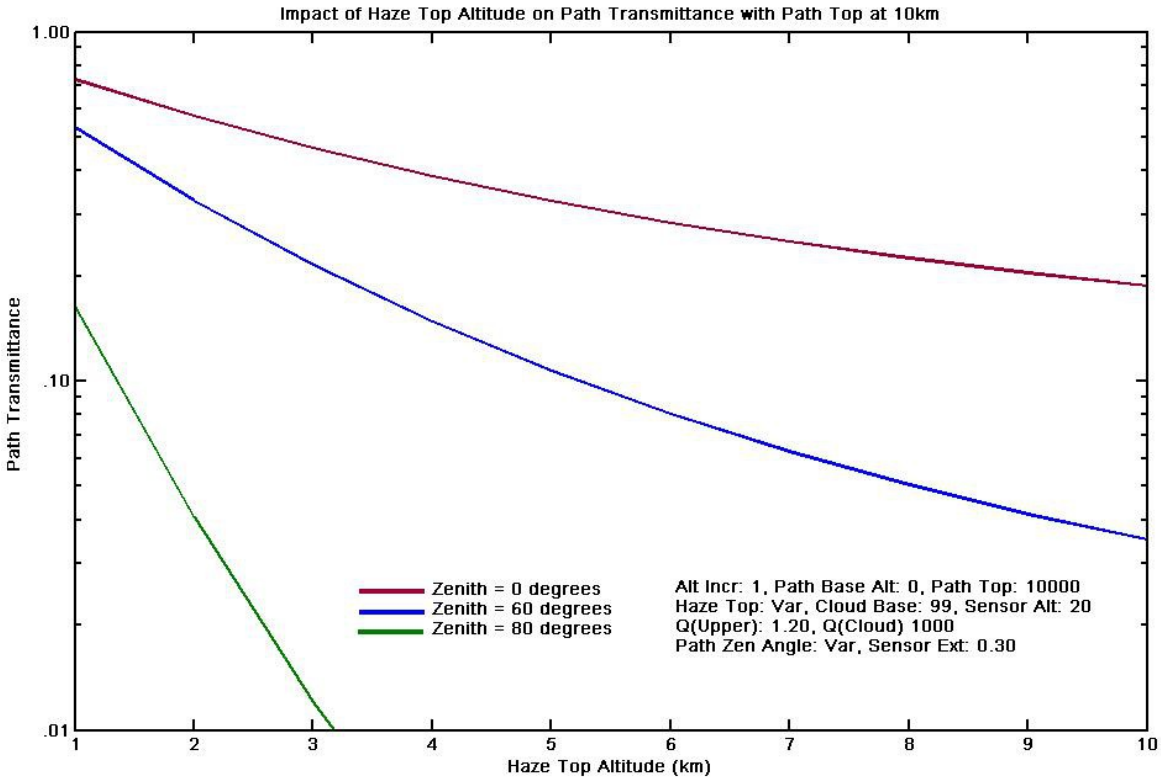

Fig. 10. Log plot showing impact of varying Haze Top for a Path Top of 10 km and for Zenith Angles 0°, 60°, and 85°

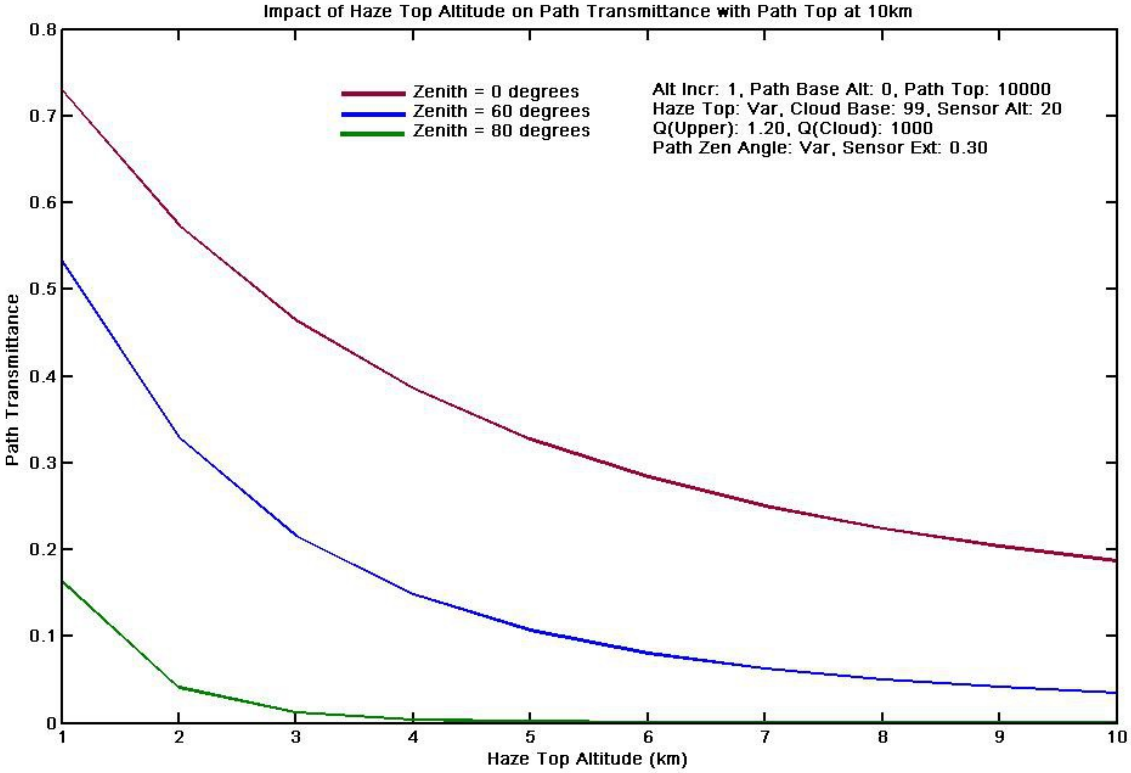

Fig. 11. Linear plot showing impact of varying Haze Top for a Path Top of 10 km and for Zenith Angles 0°, 60°, and 85°

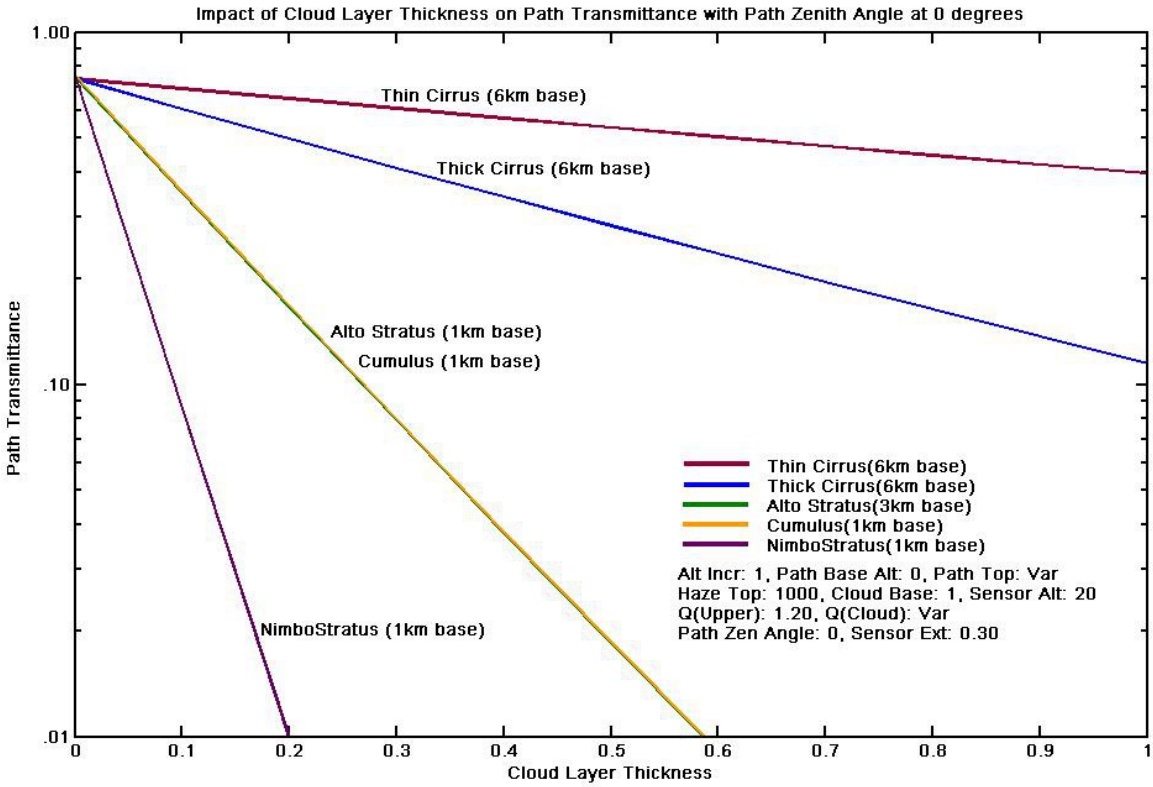

Fig. 12. Log plot showing impact of varying Cloud Layer Thickness for five cloud types at 0° zenith

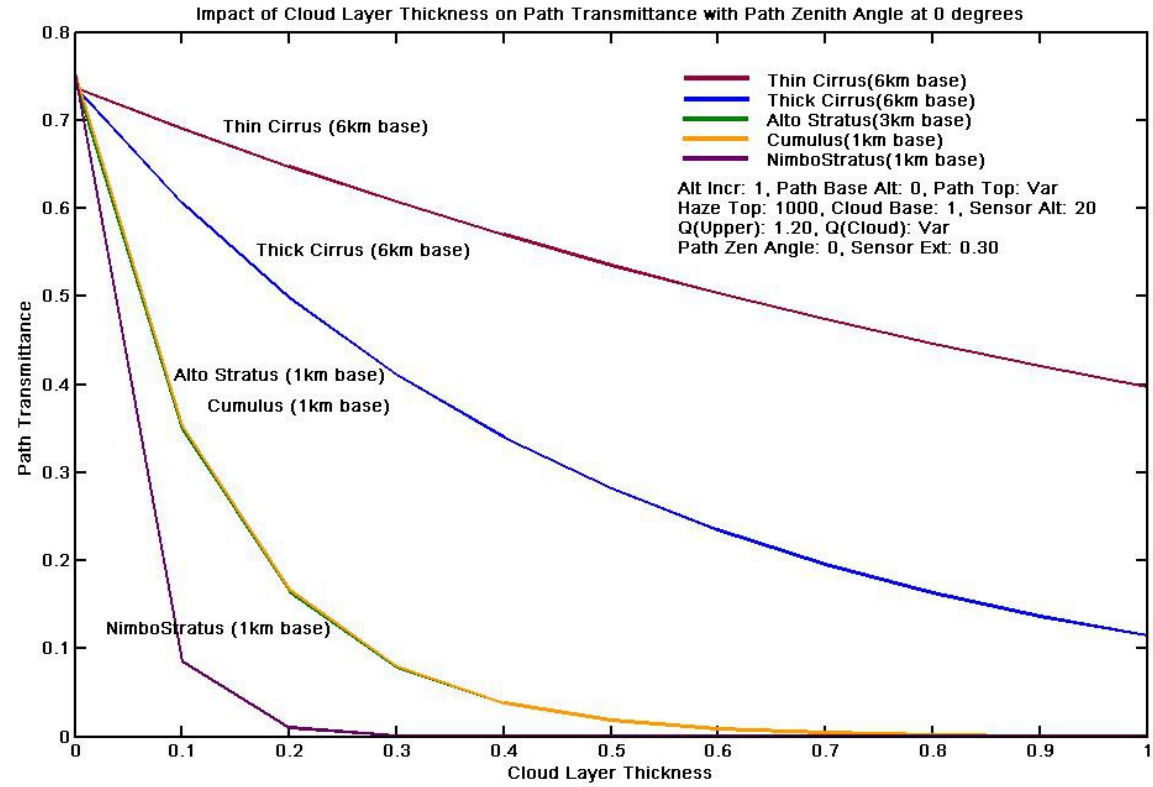

Fig. 13. Linear plot showing impact of varying Cloud Layer Thickness for five cloud types at 0° zenith

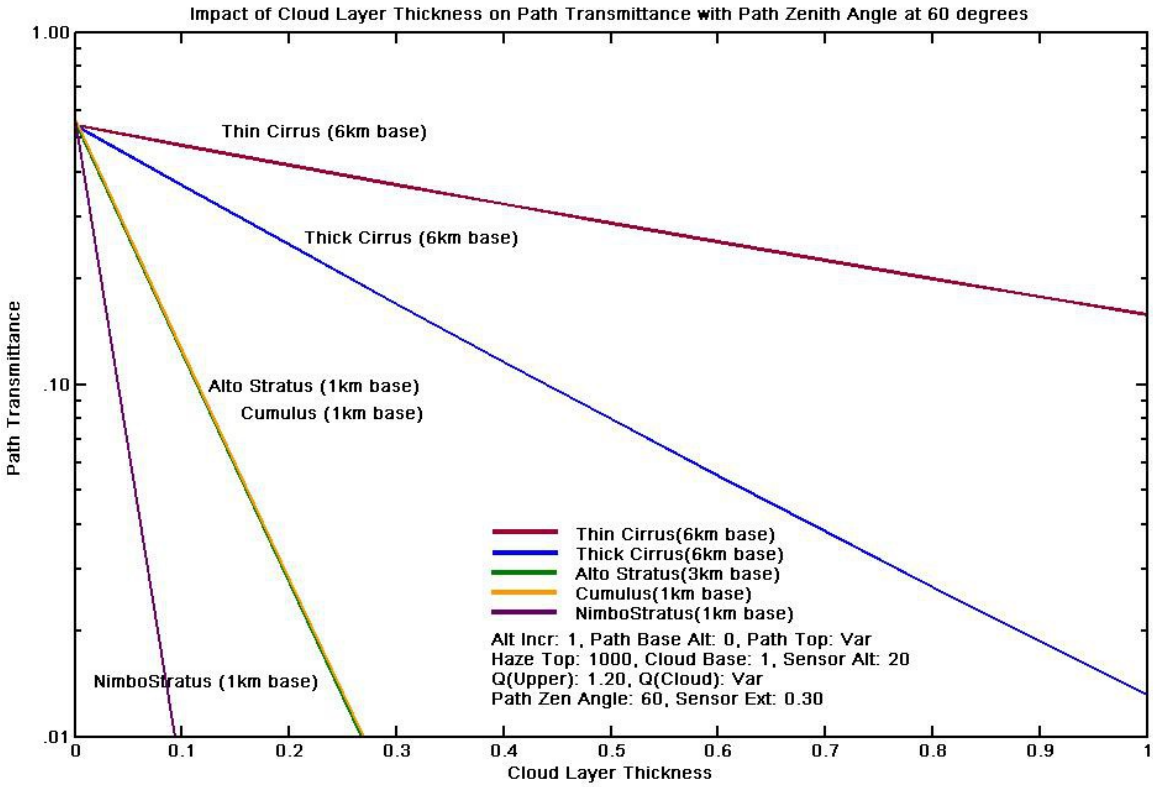

Fig. 14. Log plot showing impact of varying Cloud Layer Thickness for five cloud types at 60° zenith

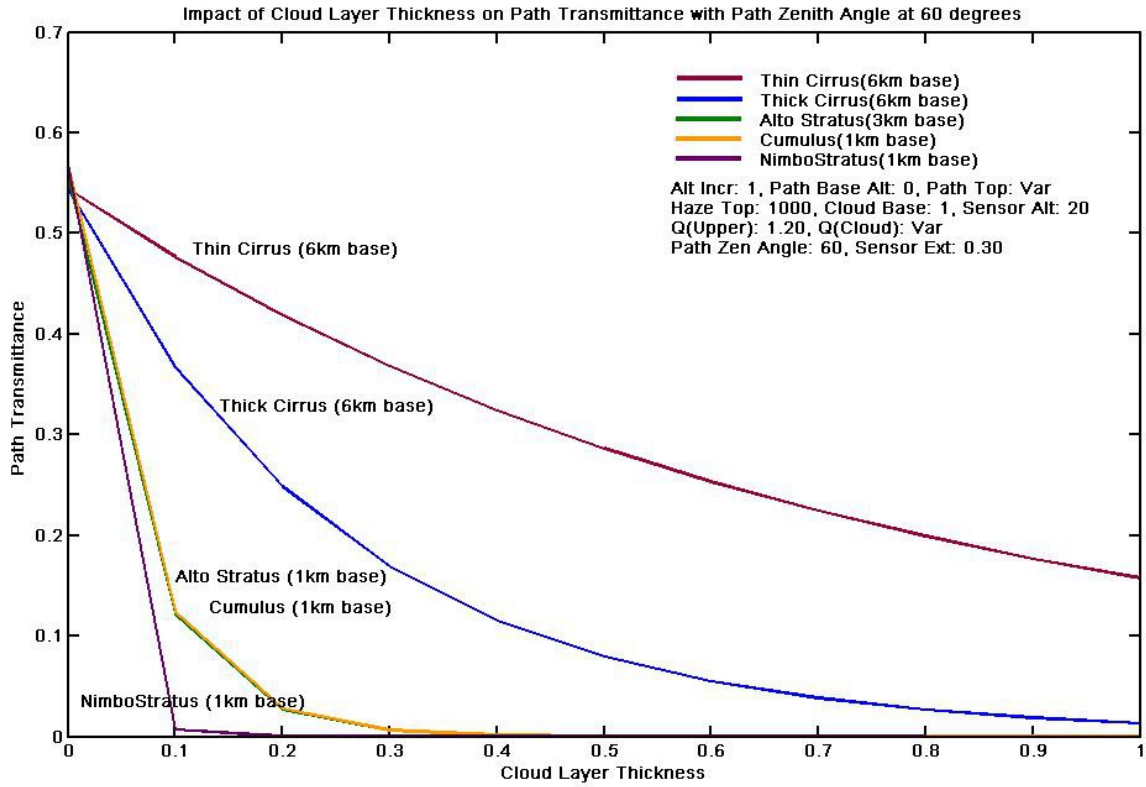

Fig. 15. Linear plot showing impact of varying Cloud Layer Thickness for five cloud types at 60° zenith

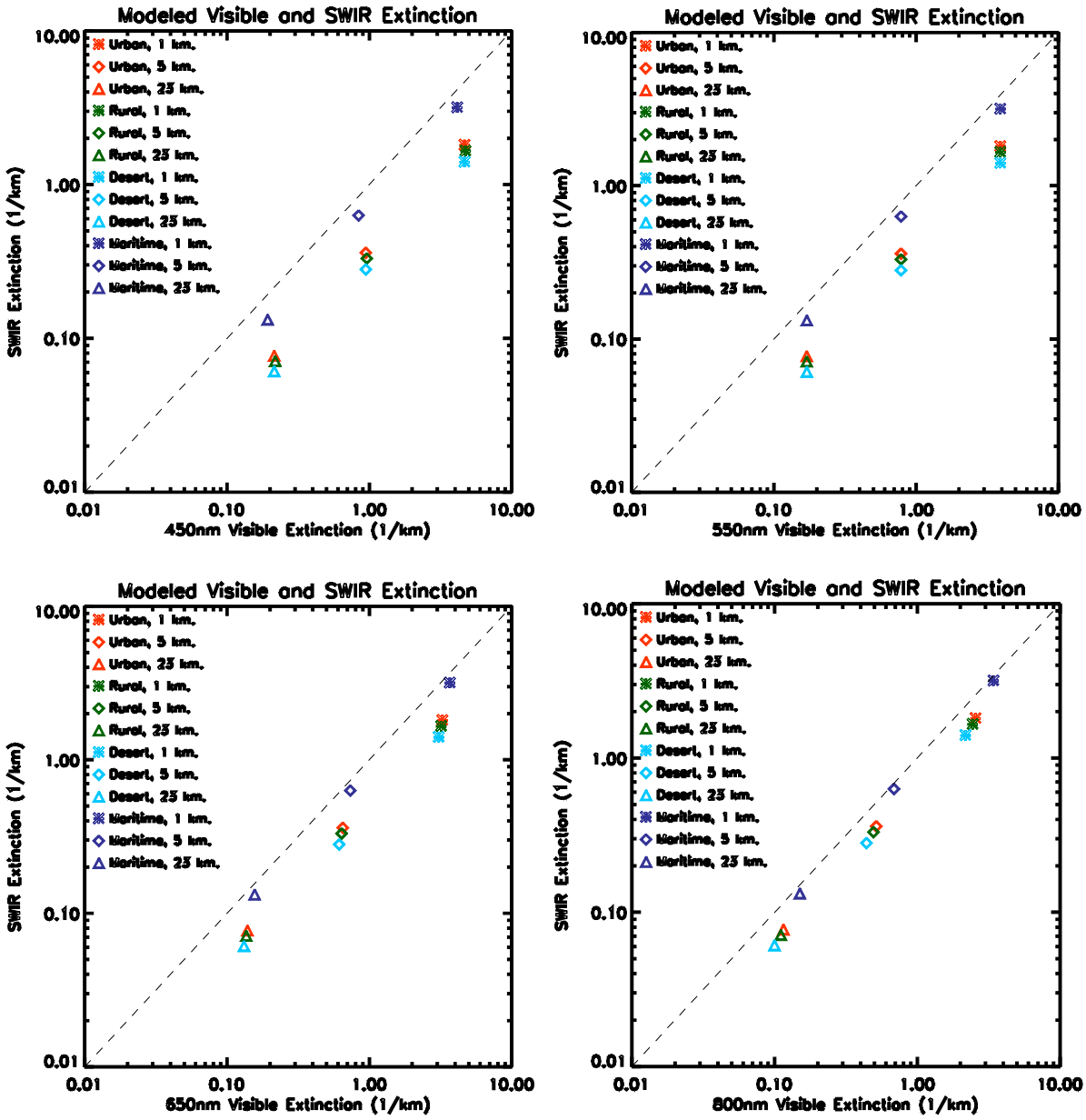

Fig. 16. Plots of MODTRAN results showing SWIR extinction at 1.064 μm as a function of modeled extinction at all four MSI wavelengths